Disruption of ST5 is associated with mental-retardation and multiple congenital anomalies

Göhring, I ; Tagariello, A ; Endele, S ; Stolt, C C ; Ghassibé, M ; Fisher, M ; Thiel, C T ; Trautmann, U ; Vikkula, M ; Winterpacht, A ; FitzPatrick, D R ; Rauch, A

Abstract: We observed a patient with a cryptic subtelomeric de novo balanced translocation 46,XY.ish t(11;20)(p15.4;q13.2) presenting with severe mental retardation, muscular hypotonia, seizures, bilateral sensorineural hearing loss, submucous cleft palate, persistent ductus Botalli, unilateral cystic kidney dysplasia and frequent infections. Fluorescence in situ hybridization mapping and sequencing of the translocation breakpoints showed that no known genes are disrupted at 20q13.2 and that ST5 (suppression of tumorigenicity 5; MIM 140750) is disrupted on 11p15.4. By quantitative PCR from different human tissues we found ST5 relatively evenly expressed in fetal tissues. ST5 expression was more pronounced in adult brain, kidney and muscle than in the corresponding fetal tissues, whereas expression in other tissues was generally lower than in the fetal tissue. Using RNA in situ hybridization in mouse we found that St5 is expressed in the frontal cortex during embryonic development. In adult mouse brain expression of St5 was especially high in the hippocampal area and cerebellum. Hence we suppose that ST5 plays an important role in central nervous system development probably due to disturbance of DENN-domain mediated vesicle formation and neurotransmitter trafficking. Thus, our findings implicate ST5 in the etiology of mental retardation, seizures and multiple congenital anomalies.

DOI: https://doi.org/10.1136/jmg.2009.069799

Disruption of *ST5* is associated with mental-retardation and multiple congenital anomalies

Ina Göhring,[1] Andreas Tagariello,[1] Sabine Endele,[1] Claus C. Stolt,[2] Michella Ghassibé,[3] Malcolm Fisher,[4] Christian T. Thiel,[1] Udo Trautmann,[1] Miikka Vikkula,[3] Andreas Winterpacht,[1] David R. FitzPatrick,[4] and Anita Rauch[1,5*]

[1]Institute of Human Genetics, Friedrich-Alexander University Erlangen-Nuremberg, 91054 Erlangen, Germany
[2]Institute of Biochemistry, Emil-Fischer Centre, Friedrich-Alexander University Erlangen-Nuremberg, 91054 Erlangen, Germany
[3]de Duve Institute, Université catholique de Louvain, B-1200 Brussels, Belgium
[4]Medical and Developmental Genetics Section, MRC Human Genetics Unit, Western General Hospital, Edinburgh EH4 2XU, United Kingdom
[5]Institute of Medical Genetics, University of Zurich, CH-8603 Schwerzenbach-Zurich, Switzerland

[*]Address for correspondence:
Anita Rauch, Prof. Dr. med.
Institute of Medical Genetics
University of Zurich
Schorenstrasse 16, CH-8603 Schwerzenbach-Zurich, Switzerland
Tel: +41-44-6557051
Email: anita.rauch@medgen.uzh.ch

Key words
Mental retardation, seizures, ST5, 11p15.4, DENN-domain

ABSTRACT
We observed a patient with a cryptic subtelomeric de novo balanced translocation 46,XY.ish t(11;20)(p15.4;q13.2) presenting with severe mental retardation, muscular hypotonia, seizures, bilateral sensorineural hearing loss, submucous cleft palate, persistent ductus Botalli, unilateral cystic kidney dysplasia and frequent infections. Fluorescence *in situ* hybridization mapping and sequencing of the translocation breakpoints showed that no known genes are disrupted at 20q13.2 and that *ST5* (suppression of tumorigenicity 5; MIM 140750) is disrupted on 11p15.4. By quantitative PCR from different human tissues we found *ST5* relatively evenly expressed in fetal tissues. *ST5* expression was more pronounced in adult brain, kidney and muscle than in the corresponding fetal tissues, whereas expression in other tissues was generally lower than in the fetal tissue. Using RNA *in situ* hybridization in mouse we found that *St5* is expressed in the frontal cortex during embryonic development. In adult mouse brain expression of *St5* was especially high in the hippocampal area and cerebellum. Hence we suppose that *ST5* plays an important role in central nervous system development probably due to disturbance of DENN-domain mediated vesicle formation and neurotransmitter trafficking. Thus, our findings implicate *ST5* in the etiology of mental retardation, seizures and multiple congenital anomalies.

INTRODUCTION

Mental retardation (MR) is defined as a significant impairment of cognitive and adaptive functions with onset before age 18 years and affects about 2-3% of the population. It occurs as an isolated trait or as part of many syndromes and despite significant improvement in the identification of underlying causes, the majority of cases currently remain without definitive diagnosis.[1] Since MR is extremely heterogeneous and occurs sporadically in most patients, identification of novel causative genes by linkage analysis is difficult. In such cases balanced chromosomal rearrangements, which occur in 0.6% of mentally retarded patients are one of the most promising sources to target particular genomic segments or genes responsible for MR or other developmental disorders in humans.[1] The phenotypic effects observed in patients with truly balanced chromosomal rearrangements can be explained by the disruption of genes or by alteration of

expression of genes residing at the chromosomal breakpoints or in close proximity to it. In this study, breakpoint mapping of a balanced de novo translocation t(11;20)(p15.4;q13.2) in a patient with MR, seizures and multiple congenital anomalies led to the identification of *ST5* as a novel gene for syndromic mental retardation.

METHODS

Fluorescence *in situ* hybridization

Region specific BAC clones for FISH mapping were selected from the NCBI and UCSC genome browsers (http://www.ncbi.nlm.nih.gov, http://www.ncbi.nlm.nih.gov). FISH analyses were performed using metaphase chromosomes prepared from lymphoblastoid cell lines. Genomic BAC DNAs were fluorescently labeled with Cy3-dCTP (Amersham Biosciences) by standard nick translation with the DIG-Nick-Translation Kit (Roche). The probes were blocked with Cot-1 DNA to suppress repetitive sequences. Metaphase spreads were hybridized at 37°C overnight with the Cy3 labeled BAC-probes and a specific FluoroX (Amersham Biosciences) labeled subtelomeric control probe (PAC probes GS-11q770-G7 or GS-20p1061-L1).[2] After post-hybrizidation washes, chromosomes were counterstained with DAPI (Serva). Images were captured on a Zeiss Axioplan 2 microscope with a CCD camera and processed with the Isis Software (Metasystems).

Long-Template PCR and Mini-FISH analyses

All Long-Template PCRs were performed with the Expand Long Template PCR-System (Roche Diagnostics) according to the recommendations of the manufacturer with primer pairs chosen from the genomic sequence of the breakpoint-spanning BAC clones. Annealing temperatures and elongation times were optimized for each primer pair. Purified long-template PCR-products (QIAquick PCR Purification Kit, Qiagen) were labeled with Cy3-dCTPs by standard nick translation as described above and FISH was performed on metaphase spreads. Hybridization time was elongated to 48 hours.

Breakpoint sequencing

Primer pairs for breakpoint-spanning PCRs were chosen from the genomic sequence of the breakpoint containing segments on chromosomes 11 and 20. Different combinations of forward and reverse primers were used to amplify a breakpoint-spanning PCR-product with the Expand 20kb^{Plus} PCR-System, dNTPack, Roche Diagnostics) according to manufacturers recommendations. We amplified the breakpoint spanning PCR product from the derivative chromosome 11 using the following primer pair Chr11-5´-TCTTCTGCCTAATGGTCAGC-3´ and Chr20-5´-CTGCAAGCCAAGAAGAGAGG-3´. The breakpoint spanning PCR product from the derivative chromosome 20 was generated with the primer pair Chr11-5´-CCATCCATCTCTCCTCATTCCTTAAGTT-3´ and Chr20-5´-CCAATTAAGATGAGAAGATCCCTCTAGGA-3´. Dye terminator cycle sequencing of the purified PCR-products was carried out using the DNA Sequencing Kit BigDye-Terminator Cycle Sequencing Ready Reaction (Applied Biosystems). Sequencing products were separated on an Applied Biosystems ABI3730 Sequencing-System. The NCBI BLAST program (http://ncbi.nlm.nih.gov/BLAST) and the UCSC BLAT program (http://genome.ucsc.edu/cgi-bin/hgBlat) were used to analyze the sequencing files.

Copy number analysis

To investigate the presence of the reported *ST5* copy number variations in well characterized control individuals, we performed long range PCR using intronic primers from intron 7 to intron 10, which generated a 3.4 kb product in 192 healthy blood donors. Copy number changes larger than 100 kb were investigated in 667 mentally healthy individuals using data generated with the Affymetrix GeneChip SNP array 6.0 and the Genotyping Console 3.0.2 software to call segments of copy number changes.

Quantification of *ST5* expression by Real Time RT-PCR

cDNAs were taken from the Human Fetal Multiple Tissue cDNA (MTC) Panel and from the Human Adult Multiple Tissue cDNA (MTC) Panel (Clontech). RT-PCR studies were performed as described previously using the *ST5* pre-designed TaqMan® Gene Expression Assay (Applied Biosystems, Hs00373572_m1), and normalized against the mean of four endogeneous controls (b-2-microglobulin, b-actin, hypoxanthine phosphoribosyltransferase 1, and RNA polymerase II).[3] Relative expression levels were compared to the mean value of *ST5* expression in fetal brain.

RNA *in situ* hybridization

Murine expression of *St5* was investigated on embryonic days 8.5, 13.5 and 15 (E8.5, E13.5, E15), in brain and kidneys of new born mice on days 6, 10 and 15 (P6, P10, P15) and in brains of 7 weeks old mice and adult mice. Tissue was OCT (TissueTek) embedded and stored at -80°C. Serial kryostat sections at 10-12 µm were fixed in 4% paraformaldehyde/PBS. A 448 bp mouse *St5* riboprobe was generated by PCR using the primers ggagactgtgggtcactactcc and aatatggtgaaggcagaagtgg and subcloning of the amplicon into the pCR4-TOPO vector (Invitrogen) as recommended by the manufacturer. The probe was labeled according to the *in vitro* transcription kit (DIG-RNA Labeling Mix, Roche) using 10 µl linearizised plasmid, 2 µl 10x Labeling Mix, 2 µl 10x transcription buffer, 1 µl RNase-inhibitor, 2 µl polymerase (T3 or T7 according to sense- or antisense-probes) and 3 µl PCR-grade water. The mix was incubated at 37°C for 2 hours. Serial sections were hybridized with digoxigenin (DIG-UTP)-labeled RNA sense and antisense probes and with a control riboprobe (*COL2A1*). Hybridization was carried out at 60°C in 50% formamide overnight. The slides were washed four times in 2x SSC, three times in 0.1x SSC (all incubations 30 min) and finally 5 minutes in PBT. Reaction was blocked with Blocking buffer (Roche Diagnostics) for 40 minutes and then the slides were incubated with AP-conjugated Anti-DIG F_{ab}-fragments (Roche Diagnostics) at 37°C for 1 hour. The slides were counterstained with toluidinblue (Roche Diagnostics). Images were captured on a MZ16 microscope (Leica) with a CCD camera (DC300, Leica) and processed with the IM-Software 1.20 (Leica).

RESULTS

Case report

The patient described here was introduced to the genetics clinic at the age of 3.5 years presenting with severe mental retardation, muscular hypotonia, seizures, bilateral sensorineural hearing loss, submucous cleft palate, persistent ductus Botalli, unilateral cystic kidney dysplasia, and a history of frequent infections. He also showed dysmorphic facial features including a high forehead, high arched, laterally placed eyebrows, broad glabella, mild hypertelorism, narrow, upslanting palpebral fissures, a small mouth with thin upper lip and everted lower lip, a broad nasal bridge and hypoplastic nasal wings. The proband was the third child of healthy, unrelated European parents. Since ultrasound examinations showed unilateral cystic kidney dysplasia prenatal cytogenetic analysis of chorionic villi specimens was performed and showed a normal karyotype. The patient was born at 38 weeks of gestation with a length of 51 cm (50^{th} centile), a weight of 3490 g ($50\text{-}75^{th}$ centile) and a head circumference of 34 cm ($25\text{-}50^{th}$ centile). He showed delayed achievement of motor milestones. At the age of 3 years and 6 month he could neither walk nor speak. At the age of 7 years the boy was able to walk with orthoses but still showed no speech. Absences and focal seizures with generalisation which were resistant to therapy were observed starting at the age of 6 month. Neither brain magnetic resonance imaging nor metabolic testing showed any abnormalities. Subtelomeric screening by fluorescence *in situ* hybridisation (FISH) using an optimized BAC/PAC set [2] showed an apparently balanced translocation, which was in combination with whole chromosome painting and high resolution GTG-banding interpreted as 46,XY.ish t(11;20)(p15;q13.3)(wcp20+,20QTEL14+,11PTEL03-,wcp11+;wcp20+,20QTEL14-,wcp11+,11PTEL03+) (Figure 1 A, B). Parental karyotypes including subtelomeric FISH studies were normal. Since it was recently shown that apparently balanced translocations may be associated with microdeletions or duplications within the breakpoint region or in independent locations,[4] we performed molecular karyotyping using an Affymetrix GeneChip Mapping 250 K Nsp SNP array. Though seven copy number variations were detected using the Nexus software (BioDiscovery), all of them were previously described as present in normal individuals according to the Database of Genomic Variants (http://projects.tcag.ca/variation/) and were therefore not of further interest. Especially we revealed no significant loss or gain of copy number at either site of the breakpoints.

Chromosomal breakpoint mapping

In order to map the translocation breakpoints at a higher DNA resolution, we selected region-specific bacterial artificial chromosome (BAC) clones from the databases. Individual BACs from the breakpoint regions were hybridized to the patient's metaphase spreads. On chromosome 11 BAC clone RP11-152H18 (8.6 Mb from pter) showed fluorescence *in situ* hybridization signals localized on both derivative chromosomes, demonstrating that it spanned the breakpoint (Figure 1 C). On Chromosome 20 the breakpoint was spanned by the BAC clone RP5-1106N18 (49.3 Mb

from pter) (Figure 1 D). In order to narrow down the resulting breakpoint regions of 161 kb on chromosome 11 and of 87 kb on chromosome 20 further breakpoint refinement was performed using "mini-FISH" probes created by amplifying 12-18 kb fragments from the breakpoint-spanning BACs via long template PCR. Amplicons were Cy3 labeled by nick translation and used for metaphase FISH. For some of the generated long template PCR amplicons FISH analysis did not result in usable signals, probably because of the repetitive sequences enclosed in this region. However, with this method it was possible to narrow the breakpoint region on the derivative chromosome 11 to a 50 kb fragment between probes Chr11-F1 and Chr11-F7 and on the derivative chromosome 20 to a 10 kb fragment between probes Chr20-F3 and Chr20-F5 (Figure 2 A). Combining the results of FISH and mini-FISH analyses we were able to refine the breakpoint on chromosome 11 from 11p15 to 11p15.4 and to change the breakpoint on chromosome 20 from 20q13.3 to 20q13.2.

We made an effort to generate breakpoint-spanning long-template PCR products from both derivative chromosomes. By sequencing these PCR products we exactly mapped the breakpoint on chromosome 11 between position 8,729,572 and 8,729,575 bp (UCSC hg18) and on chromosome 20 between position 49,349,869 and 49,349,871 bp with loss of 3 bp on each chromosome (Figure 2 B). The chromosomal break on chromosome 20 did not occur within any known or putative genes, with the closest gene residing at a distance of 91 kb. Although the possibility of position effects on nearby genes has to be considered, so far these genes have not been associated with mental retardation or malformations. In contrast the breakpoint on chromosome 11 was located within intron 4 in the 5-prime UTR region of the *ST5*-gene, 725 bp before the first coding exon 5 (Figure 3 A). Hence we assumed that the complete coding region of this gene was separated from its promoter region.

Expression analyses of *ST5*

To further elucidate the involvement of *ST5* in the patients' phenotype we investigated its expression in fetal and adult human tissues by quantitative RT-PCR as well as by RNA *in situ* hybridization on mouse sections. RT-PCR studies were performed using the *ST5* pre-designed TaqMan® Gene Expression Assay (ABI, Hs00373572_m1), which recognizes exons seven and eight and thus detects all three isoforms. Relative expression levels were compared to the mean value of *ST5* expression in fetal brain. In accordance with the literature we found *ST5* not expressed in lymphoblasts in a relevant level.[5] In RNA from human fetal tissues we saw a relatively uniform expression pattern. In contrast, expression in most adult tissues was lower than in the corresponding fetal tissues, the highest levels were found in adult brain, kidney and skeletal muscle with 2.5 to 3 times higher expression levels compared to the respective fetal tissues (Figure 3 A).

In addition we examined murine expression of *St5* by RNA *in situ* hybridization at embryonic days 8.5, 13.5 and 15 (E8.5, E13.5, E15) as well as in brain and kidneys of new born mice on days 6, 10 and 15 (P6, P10, P15) and in brains of 7 weeks old mice and adult mice. The generated riboprobe detects the mouse homologue of human exon 6, which contains the ABL1-interacting domain and thus is specific for isoforms 1 and 3. In accordance with the human RT-PCR studies, we found increased expression of *St5* during development (Figure 4 A-D and 5). Prenatally, the strongest hybridization signals were seen in the neuroepithelium of the telencephalon, midbrain and hindbrain of an E9.5 embryo (Figure 5 A-C). Specific expression could also be detected in the developing neural region of the telencephalon, midbrain and hindbrain as well as in the atrial walls and in a regular pattern of stripes in the regions between nerves from the dorsal root ganglia of an E11.5 embryo (Figure 5 D-H). Expression was also seen in neurons within the ventricular and the marginal zone of the frontal cortex of an E15 embryo (Figure 4 C1) and could also be detected in various other tissues including developing tubular structures of the kidneys and the hard palate (Figure 4 C2-C3, E-H). Postnatally, *St5* was expressed ubiquitously in the mouse brain, but particularly high signals were found in the cortex, in the hippocampal formation and in the cerebellum whereas the corpus callosum showed no expression (Figure 4 I-O).

Mutational analysis

We had no patient with the same phenotype available for mutational analysis, but assuming clinical variability we performed *ST5* mutational analysis in a total of 220 patients with unclassified mental retardation, of whom 96 had moderate mental retardation, 96 had severe mental retardation and 28 had mental retardation in combination with any of the further symptoms of cleft palate, deafness, kidney dysplasia, or seizures. Since we found only inherited missense-mutations in these patients, the *ST5* related phenotype seems to be quite specific. We also sequenced *ST5* in the translocation

patient to exclude a mutation on the second allele.

Copy number analysis

Neither Affymetrix 6.0 array analysis nor long-range PCR within the *ST5*-gene revealed any copy number variation in the investigated control individuals.

DISCUSSION

ST5 (suppression of tumorigenicity 5; MIM 140750) was identified by its ability to suppress the tumorigenicity of HeLa cells in nude mice. It spans 217,600 bp and consists of 4 non-coding and 19 coding exons. Three isoforms of *ST5* are described, all of which contain at their 3' end a DENN-domain (differentially expressed in neoplastic versus normal cells) region.[6, 7] Other DENN-domain containing proteins are the Rab-proteins, which belong to the Ras-superfamily of GTPases. It is supposed that these domains are crucial for calcium-dependent exocytosis and therefore are closely linked to neurotransmitter release in neurons.[8] *Rab3GEP* knock-out mice suffer from seizures and show a distinct decrease in neurotransmitter release as well as significant reduction in the number of synaptic vesicles.[9] Of note, mutations in the human *RABGDIA*-Gen (RAB GDP-DISSOCIATION INHIBITOR, ALPHA) lead to X-linked mental retardation (X-linked non-specific mental retardation MRX; MIM 309541, http://www.ncbi.nlm.nih.gov/Omim). This gene is also known to play a role in vesicle formation and transmitter release. It was also shown that DENN-domains are able to activate the MAPK1/ERK2 signaling pathway which promotes cell growth and cell division.[9] *ST5* exon 6, which is spliced out in isoform 2, codes for an ABL1 interacting region.[10, 11, 12] Therefore only isoforms 1 and 3 are capable of binding the SH3-domain of cABL1-kinase. While isoform 1 stimulates the activation of the MAPK1/ERK2 pathway, isoform 3 inhibits the interaction between isoform 1 and ABL1 and thus decreases MAPK1/ERK2-activation.[5, 12] Co-expression of both *ST5* isoforms is likely to maintain the default level of ERK2-activation, since tumor cells, which are lacking this cell growth regulating function don't express isoform 3.[5] These findings suggest that *ST5* probably plays a role in cell growth and cell division, cytoskeletal organization and tumorigenesis as well as in formation of synaptic vesicles and exocytosis.

Disruption of the *ST5* gene in our patient likely results in haploinsufficiency, but we had no patient material suitable to prove diminished expression since *ST5* is not expressed in relevant levels in lymphoblasts.[5] Notably, a patient with a large genomic deletion including the *ST5* gene was reported with a similar phenotype as our patient, namely severe mental retardation, persistent hypotonia, agenesis of corpus callosum, cleft soft palate, hyperthermic convulsions, microcephaly, facial dysmorphism and chronic otitis media.[13] Furthermore there are several recent reports showing that apparently dominant single gene mutations and deletions in different genes are associated with severe phenotypes including mental retardation and malformations.[14, 15] In the common variation databases one can find at least three reported variations within *ST5*, one 225 kb CNV that impinges on intron 4, an 895 bp Indel affecting intron 8 and an 1921 bp Indel affecting intron 9.[16, 17] Redon et al. reported the 225 kb CNV in one of 270 control samples whereas we haven't found this aberration in 667 mentally normal control individuals analyzed with an Affymetrix GeneChip SNP array 6.0 (unpublished data). Furthermore we investigated 192 healthy control individuals by long-range PCR with reference to the published Indels affecting introns 8 and 9 and revealed neither deletion nor insertion. In addition, by mutational analysis of 220 patients with mental retardation we only detected a few, mostly silent base pair exchanges. Each of the few missense variants detected were proven to be inherited from a healthy parent. Taken together, these findings provide evidence that neither the reported copy number variations nor mutations in the *ST5*-gene are tolerated in the normal population but should lead to a specific phenotypic effect.

Expression analyses by quantitative RT-PCR in fetal and adult human tissues showed *ST5* as relatively uniformly expressed in fetal tissues. *ST5* expression was more pronounced in adult brain, kidney and muscle than in the corresponding fetal tissues. With RNA *in situ* hybridization we were able to show, that *St5* is expressed in the frontal cortex during mouse embryonic development and in the hippocampal area and cerebellum of adult mouse brain, as well as in developing tubular structures of the kidneys and the hard palate. Thus, both, human and mouse expression patterns of *St5* perfectly reflects the malformation pattern and brain dysfunction observed in our patient with *ST5* disruption.

In summary we suggest that *ST5* like other DENN-domain containing Rab-proteins plays a crucial

role in brain development, probably due to the assumed function in vesicle trafficking and neurotransmitter release. The latter could account not only for seizures and mental retardation, but also for sensorineural deafness, which was also seen in our patient. The cleft palate and the kidney dysplasia in our patient, however, may be explained by other regulatory functions of *ST5* in the MAPK1/ERK2 signalling pathway.

FUNDING

This study was supported by the IZKF grant E5 to A. R.. M. V. was supported by a grant from the F.R.S.-FNRS. This work was performed as part of our research study addressing the genetics of mental retardation, which was approved by the research ethics committee of the Medical Faculty of the University of Erlangen-Nuremberg.

Competing Interest: None to declare.

REFERENCES

1 Rauch A, Hoyer J, Guth S*, et al.* Diagnostic yield of various genetic approaches in patients with unexplained developmental delay or mental retardation. *Am J Med Genet A* 2006;**140**(19):2063-74.

2 Knight SJ, Lese CM, Precht KS*, et al.* An optimized set of human telomere clones for studying telomere integrity and architecture. *Am J Hum Genet* 2000;**67**(2):320-32.

3 Thiel CT, Mortier G, Kaitila I*, et al.* Type and level of RMRP functional impairment predicts phenotype in the cartilage hair hypoplasia-anauxetic dysplasia spectrum. *Am J Hum Genet* 2007;**81**(3):519-29.

4 De Gregori M, Ciccone R, Magini P*, et al.* Cryptic deletions are a common finding in "balanced" reciprocal and complex chromosome rearrangements: a study of 59 patients. *J Med Genet* 2007;**44**(12):750-62.

5 Hubbs AE, Majidi M, Lichy JH. Expression of an isoform of the novel signal transduction protein ST5 is linked to cell morphology. *Oncogene* 1999;**18**(15):2519-25.

6 Hubbard TJ, Aken BL, Beal K*, et al.* Ensembl 2007. *Nucleic Acids Res* 2007;**35**(Database issue):D610-7.

7 Maglott D, Ostell J, Pruitt KD*, et al.* Entrez Gene: gene-centered information at NCBI. *Nucleic Acids Res* 2005;**33**(Database issue):D54-8.

8 Yamaguchi K, Tanaka M, Mizoguchi A*, et al.* A GDP/GTP exchange protein for the Rab3 small G protein family up-regulates a postdocking step of synaptic exocytosis in central synapses. *Proc Natl Acad Sci U S A* 2002;**99**(22):14536-41.

9 Levivier E, Goud B, Souchet M*, et al.* uDENN, DENN, and dDENN: indissociable domains in Rab and MAP kinases signaling pathways. *Biochem Biophys Res Commun* 2001;**287**(3):688-95.

10 Lichy JH, Majidi M, Elbaum J*, et al.* Differential expression of the human ST5 gene in HeLa-fibroblast hybrid cell lines mediated by YY1: evidence that YY1 plays a part in tumor suppression. *Nucleic Acids Res* 1996;**24**(23):4700-8.

11 Majidi M, Gutkind JS, Lichy JH. Deletion of the COOH terminus converts the ST5 p70 protein from an inhibitor of RAS signaling to an activator with transforming

activity in NIH-3T3 cells. *J Biol Chem* 2000;**275**(9):6560-5.
12 Majidi M, Hubbs AE, Lichy JH. Activation of extracellular signal-regulated kinase 2 by a novel Abl-binding protein, ST5. *J Biol Chem* 1998;**273**(26):16608-14.
13 Kleczkowska A, Fryns JP, Jaeken J, *et al.* Complex chromosomal rearrangement involving chromosomes 11, 13 and 21. *Ann Genet* 1988;**31**(2):126-8.
14 Mencarelli M, Spanhol-Rosseto A, Artuso R, *et al.* Novel FOXG1 mutations associated with the congenital variant of Rett syndrome. *J Med Genet* 2009.
15 Zweier C, Peippo MM, Hoyer J, *et al.* Haploinsufficiency of TCF4 causes syndromal mental retardation with intermittent hyperventilation (Pitt-Hopkins syndrome). *Am J Hum Genet* 2007;**80**(5):994-1001.
16 Mills RE, Luttig CT, Larkins CE, *et al.* An initial map of insertion and deletion (INDEL) variation in the human genome. *Genome Res* 2006;**16**(9):1182-90.
17 Redon R, Ishikawa S, Fitch KR, *et al.* Global variation in copy number in the human genome. *Nature* 2006;**444**(7118):444-54.

FIGURES

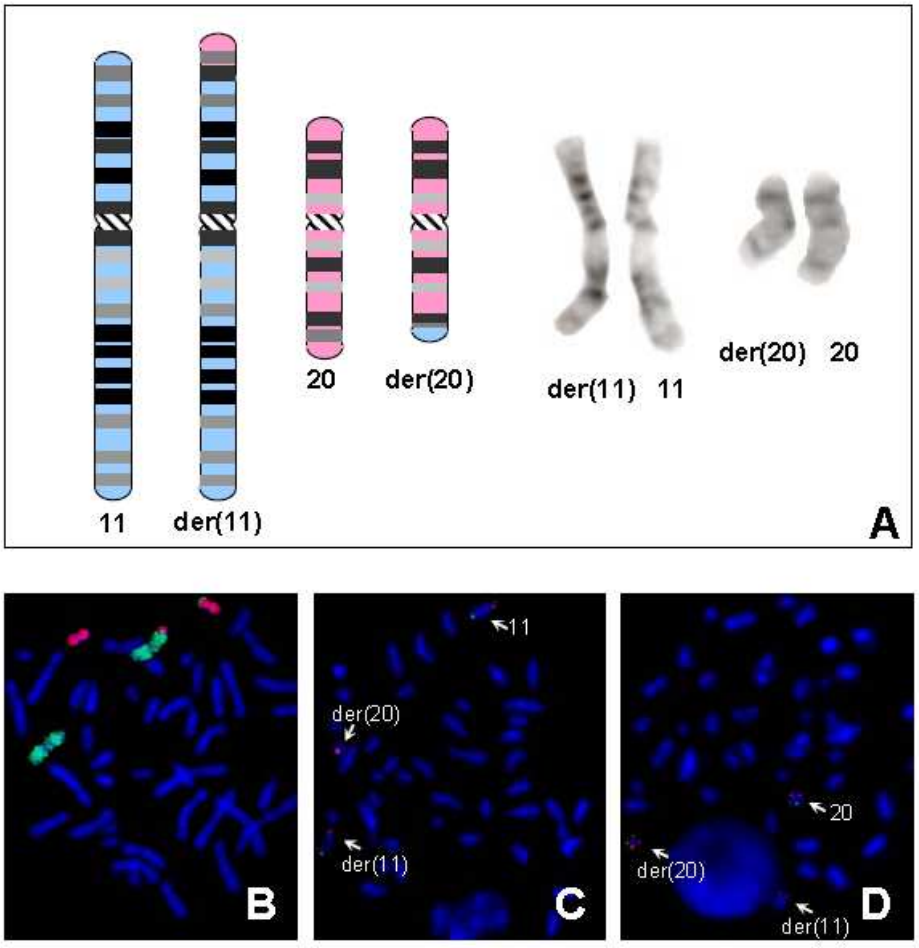

Figure 1
Subtelomeric screening and cytogenetic analysis in our patient revealed a cryptic subtelomeric translocation with the karyotype 46,XY,t(11;20)(p15.4;q13.2). The partial karyogram and ideogram is shown (A). Additionally chromosome painting using libraries for chromosome 11 (green) and 20 (red) was performed (B). For mapping of the translocation breakpoints, FISH was performed with BAC clones. BAC clones RP11-152H18 (red) on chromosome 11 (with 11qter-probe, green) (C) and RP5-906P16 (red) on chromosome 20 (with 20pter-probe, green) (D) showed hybridization signals localized on both derivative chromosomes, demonstrating that they spanned the breakpoint.

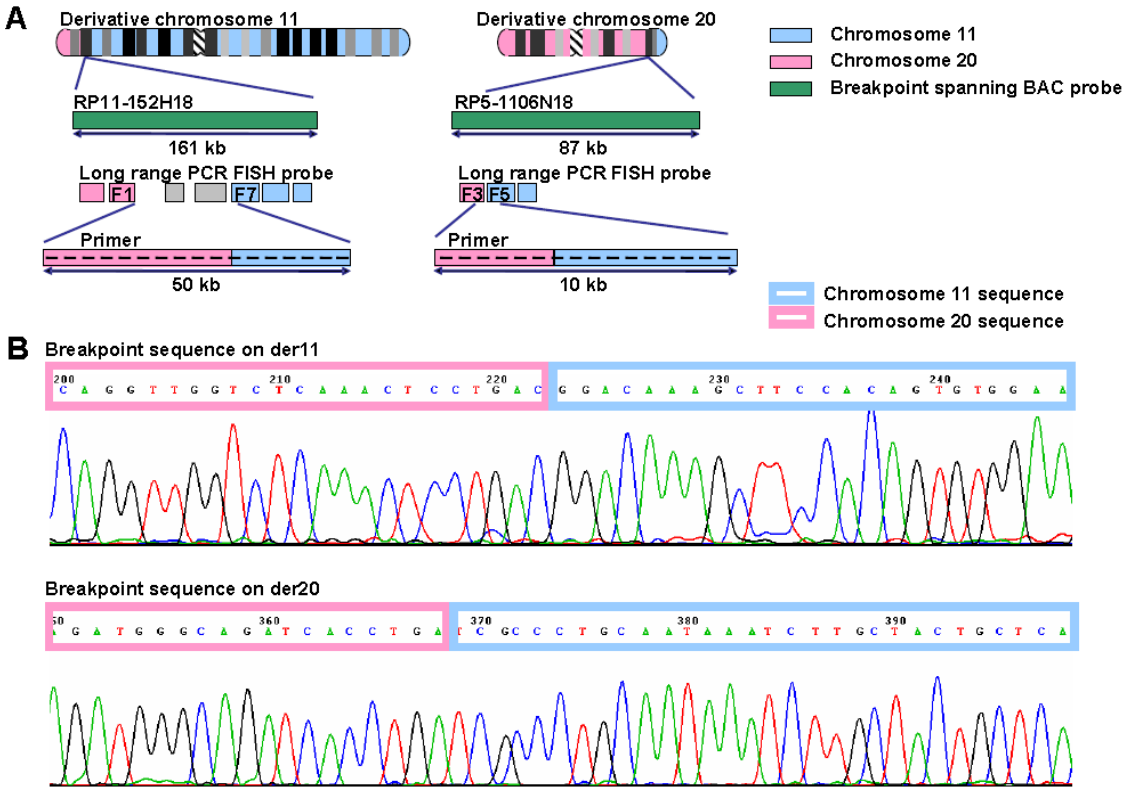

Figure 2
FISH studies narrowed the breakpoint regions to a 161 kb region on chromosome 11 and to an 87 kb region on chromosome 20 (A). “Mini-FISH” probes were created from the breakpoint-spanning BACs via long template PCR. Therewith it was possible to narrow the breakpoint region on the derivative chromosome 11 to a 50 kb fragment between probes F1 and F7. We obtained signals on chromosome 20 with probe Chr11-F1 indicating that this probe is translocated whereas probe Chr11-F7 was not translocated. For the grey illustrated “mini-FISH” probes we were not able to achieve usable results from the FISH analysis. On the derivative chromosome 20 we narrowed the breakpoint to a 10 kb fragment between probes Chr20-F3 and Chr20-F5. While we found probe Chr20-F3 not to be translocated, probe Chr20-F5 showed signals on chromosome 11, demonstrating that this probe is translocated. Finally we exactly mapped the breakpoints by sequencing of breakpoint-spanning long-template PCR products from both derivative chromosomes (B).

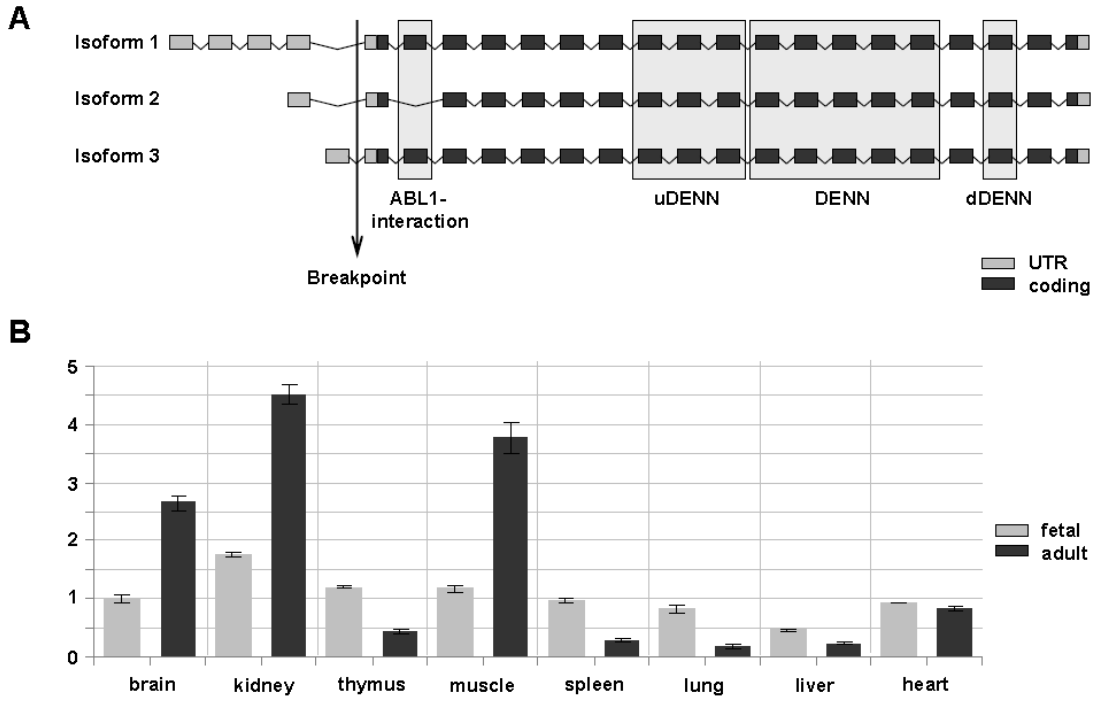

Figure 3
The breakpoint (vertical arrow) on chromosome 11 is located within intron 4 in the 5-prime UTR region of the *ST5*-gene, 725 bp before the first coding exon 5 (A), indicating that the complete coding region of *ST5* is separated from its promoter region. *ST5* spans 217.600 bp and consists of 4 non-coding and 19 coding exons. Three isoforms of *ST5* are described, all containing a DENN-domain region 3-prime. Two *ST5*-transcripts also include an ABL1-interacting-region. Expression analysis of *ST5* with quantitative PCR on commercially available cDNA panels showed relatively even expression in fetal tissues (B). In adult brain, kidney and muscle *ST5* expression was much higher than in the corresponding fetal tissues, whereas expression in other tissues was generally lower than in the respective fetal tissue.

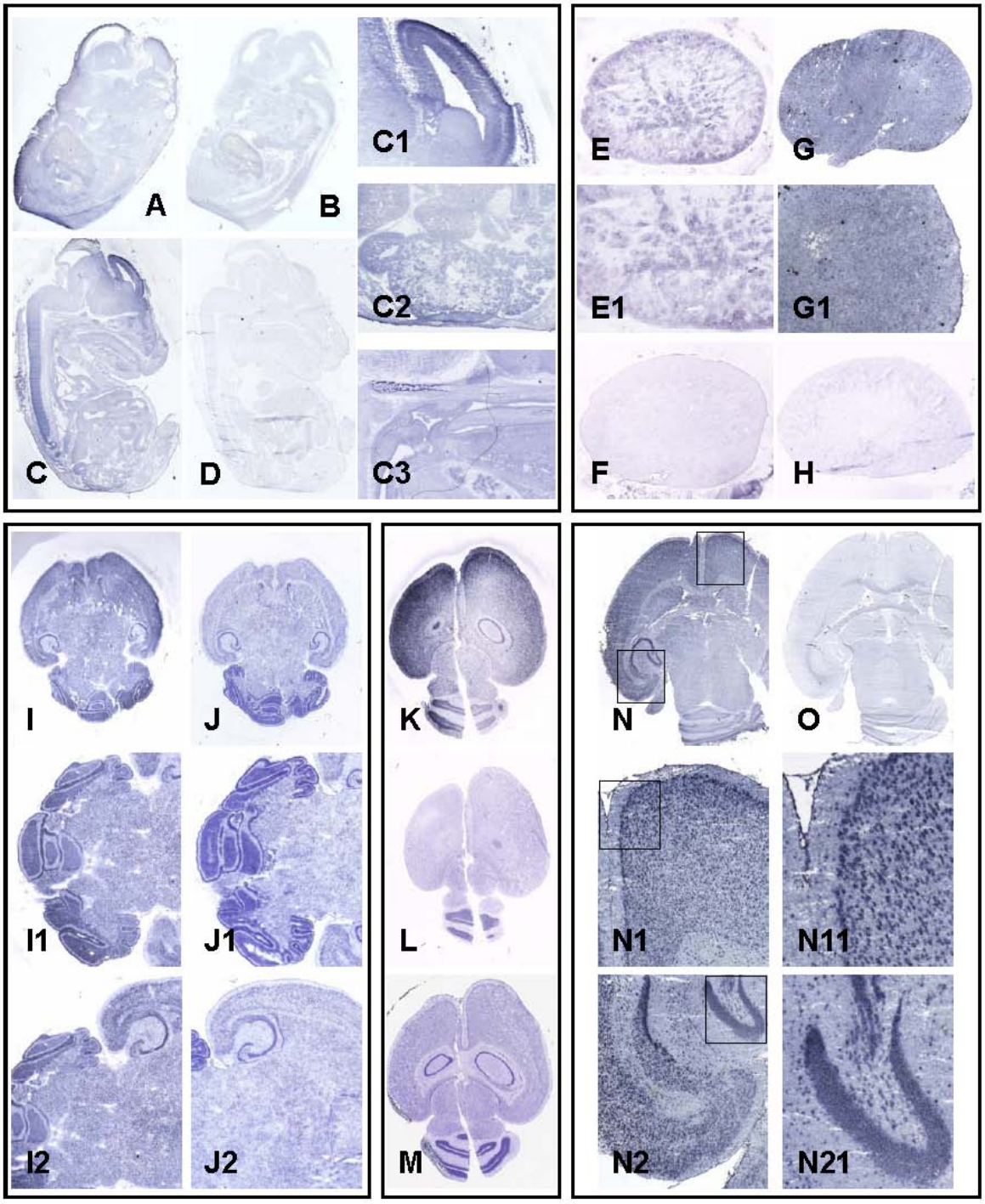

Figure 4
RNA *in situ* hybridization (ISH) on E13.5 mouse embryos with a *St5* riboprobe (A) in comparison to a negative control (B) showed no significant expression. On embryonic day 15.5, however, ISH with a *St5* riboprobe (C) in comparison to a negative control (D) indicates, that *St5* is expressed in the ventricular and the marginal zone of the frontal cortex (C1), as well as in the kidney (C2) and in the palate (arrow) (C3). *St5* is also expressed in the developing tubular structures of the kidneys of a newborn mouse (E) in comparison to a negative control (F) and of the kidneys of a 15 days old mouse (G) in comparison to the negative control (H). (E1) and (G1) are showing higher magnification of pictures (E) and (G). Pictures (I) and (J) are showing ISH with the *St5* riboprobe (I) in comparison to a neuron-specific Nissl staining (J) of a P6 mouse, demonstrating expression of *St5* especially in neurons. (I1) and (J1) are showing the cerebellum and (I2) and (J2) the hippocampal regions under higher magnification. We also examined the brain of a 7 week old mouse with our *St5* riboprobe (K), a negative control (L) and with a Nissl staining (M) as well as the brain of an adult mouse with the *St5* riboprobe (N) and a negative control (O). Signals are

basically located in the cortex (N1) and in the gyrus dendatus (N2). (N11) and (N21) are showing higher magnification of pictures (N1) and (N2).

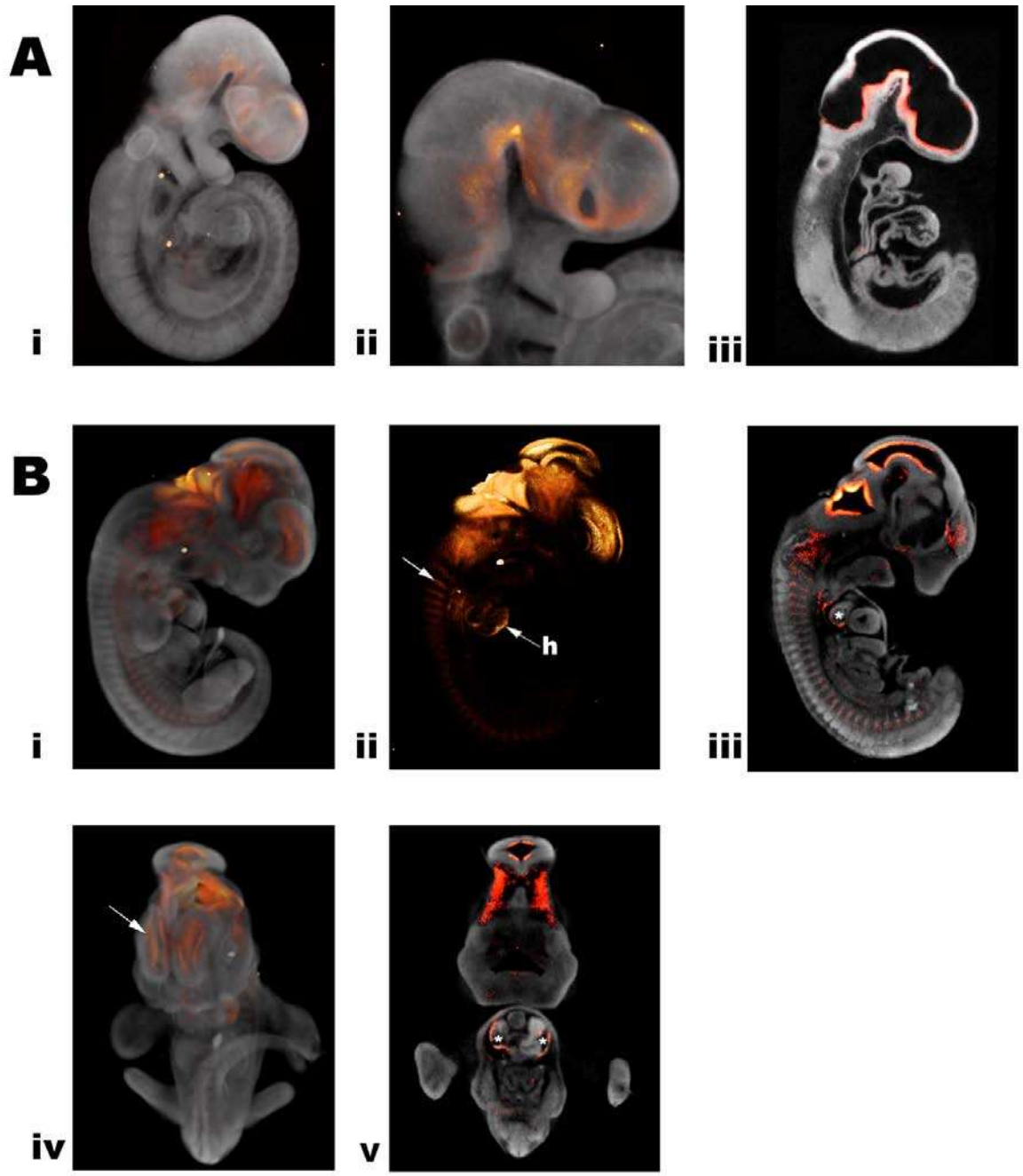

Figure 5
A volume rendering of an OPT scan of a day 9.5 *St5 in situ*, expression is rendered as red at low expression levels and yellow at higher levels. The anatomy of the embryo is rendered in a greyscale colourscheme (A). The same rendering with a sectional cut removing the right half of the embryo, this shows clearer detail of the expression of *St5* in the neuroepithelium of the midbrain and telencephalon (B). A sagittal section through the reconstructed day 9.5 embryo showing *St5* expression in the neuroepithelium of the telencephalon, midbrain and hindbrain (C). A volume rendering of an OPT scan of a day 11.5 embryo, *ST5* expression can be seen in the developing neural region, the heart and in a regular pattern of stripes down the body axis (D). A rendering of the signal alone allows greater appreciation of the expression in the heart (marked with an arrowed h), which seems to be in the left and right atria, and the regular striped pattern of expression (arrow) (E). A sagittal section through the reconstructed day 11.5 embryo showing *St5* expression in the heart, telencephalon, midbrain and hindbrain (F). Expression in the heart is seen in the left atrial chamber wall (marked by *). Expression is also visible in stripes in the regions between

nerves from the dorsal root ganglia. An oblique view of the volume rendering highlighting expression around the lateral ventricles (arrow) (G). A coronal section showing expression in the midbrain, cerebral mesenchyme and the right and left atrial walls (marked by*) (H).